



Quartz on Silicon

C. Jeffrey Brinker and Paul G. Clem

Science **340**, 818 (2013);

DOI: 10.1126/science.1236752

This copy is for your personal, non-commercial use only.

If you wish to distribute this article to others, you can order high-quality copies for your colleagues, clients, or customers by [clicking here](#).

Permission to republish or repurpose articles or portions of articles can be obtained by following the guidelines [here](#).

The following resources related to this article are available online at www.sciencemag.org (this information is current as of May 14, 2014):

Updated information and services, including high-resolution figures, can be found in the online version of this article at:

<http://www.sciencemag.org/content/340/6134/818.full.html>

A list of selected additional articles on the Science Web sites **related to this article** can be found at:

<http://www.sciencemag.org/content/340/6134/818.full.html#related>

This article **cites 14 articles**, 3 of which can be accessed free:

<http://www.sciencemag.org/content/340/6134/818.full.html#ref-list-1>

This article appears in the following **subject collections**:

Materials Science

http://www.sciencemag.org/cgi/collection/mat_sci

and identity. Evidence from *in vitro* studies demonstrated that human embryonic stem cells depend on basic fibroblast growth factor (bFGF) signaling. bFGF stimulates fibroblast-like support cells to produce insulin-like growth factor-2 (IGF-2), a factor sufficient to maintain human embryonic stem cell cultures (7). Similarly, neonatal spermatogonial stem cell pluripotency is maintained by the secretion of IGF-1 by Leydig support cells *in vitro* (8). In the mouse small intestine, IGF-1 is expressed in the subepithelial muscle cells (9), suggesting that mammalian intestinal growth may be regulated by a mechanism similar to that observed in *Drosophila*.

Vertebrate niche cells can relay a variety of stimuli through the insulin signaling cascade. Cone photoreceptor cells in the teleost retina produce IGF-1 in a time-of-day-dependent cycle. Application of IGF-1 increases the proliferation of rod progenitor cells *in vivo*, with the greatest sensitivity at night, coinciding with peak endogenous IGF-1 expression. Conversely, blocking the IGF-1 receptor, which is expressed on the rod progenitor cells, decreases their proliferation (10). Thus, localized insulin signaling can be controlled by nonmetabolic stimuli and may contribute to progenitor cell response to diverse external stimuli.

Local insulin also plays a role in mediating the proliferation of progenitor cells in response to tissue damage. In rats, induction of focal ischemia causes neuronal cell death. After ischemia, brain astrocytes (a type of glial cell) near the damaged area produce IGF-1, promoting proliferation of neighboring neural progenitors in the dentate gyrus of the adult rat hippocampus (11). Forced expression of IGF-1 in astrocytes promotes localized overgrowth of the brain in rodents (11), whereas direct infusion of IGF-1 into specific brain regions can induce neurogenesis in healthy adult mammalian brains (12). This parallels the role of glial-derived insulin in increasing neural stem cell proliferation in *Drosophila* (4, 5). Other stimuli, including exercise, also promote neurogenesis in the proliferative subventricular zone and dentate gyrus regions of the adult mouse brain, although this appears to be through systemic IGF-1 signaling (13, 14).

The discovery that stem cells are sensitive to locally produced insulin could open new avenues in the use of IGFs to activate particular stem cell populations after tissue damage or disease. The cerebrospinal fluid provides access for cerebral cortical progenitor cells in the mouse brain to insulin-like peptides (15). Infusion of insulin-like peptides into this fluid or into particular brain regions may

allow moderation of the effects of injury or neurodegeneration.

Differences in local versus systemic signaling under caloric restriction may favor the maintenance rather than proliferation of stem cell pools. This may help to explain the apparent contradiction that, although reduced insulin signaling increases life span in mammals and invertebrates, insulin signaling has a neuroprotective effect in the central nervous system (16).

Several key questions are yet to be answered about local insulin signaling, including how systemic signals are functionally coupled to niche insulin signals, how different niche signals integrate to control stem cell behavior, and how local insulin signaling changes in aging and disease. Understanding these interactions will enable a greater understanding of stem cell dynamics in response to external signals and metabolic state.

References

1. J. S. Britton, B. A. Edgar, *Development* **2158**, 2149 (1998).
2. D. S. Andersen, J. Colombani, P. Léopold, *Trends Cell Biol.* 10.1016/j.tcb.2013.03.005 (2013).
3. C. Géminard, E. J. Rulifson, P. Léopold, *Cell Metab.* **10**, 199 (2009).
4. J. M. Chell, A. H. Brand, *Cell* **143**, 1161 (2010).
5. R. Sousa-Nunes, L. L. Yee, A. P. Gould, *Nature* **471**, 508 (2011).
6. L. E. O'Brien, S. S. Soliman, X. Li, D. Bilder, *Cell* **147**, 603 (2011).
7. S. C. Bendall *et al.*, *Nature* **448**, 1015 (2007).
8. Y.-H. Huang *et al.*, *FASEB J.* **23**, 2076 (2009).
9. J. B. Pucilowska *et al.*, *Am. J. Physiol. Gastrointest. Liver Physiol.* **279**, G1307 (2000).
10. C. A. Zygarr, S. Colbert, D. Yang, R. D. Fernald, *Brain Res. Dev. Brain Res.* **154**, 91 (2005).
11. P. Ye *et al.*, *J. Neurosci. Res.* **78**, 472 (2004).
12. M. A. Aberg *et al.*, *J. Neurosci.* **20**, 2896 (2000).
13. H. van Praag *et al.*, *Nature* **415**, 1030 (2002).
14. J. L. Trejo *et al.*, *J. Neurosci.* **21**, 1628 (2001).
15. M. K. Lehtinen *et al.*, *Neuron* **69**, 893 (2011).
16. N. A. Bishop, T. Lu, B. A. Yankner, *Nature* **464**, 529 (2010).

10.1126/science.1238525

MATERIALS SCIENCE

Quartz on Silicon

C. Jeffrey Brinker^{1,2} and Paul G. Clem²

The integration of quartz with silicon may provide a route to fabricate advanced piezoelectric devices.

The on-chip integration of piezoelectric quartz would be highly beneficial for chemical sensing and accurate timing circuits. However, to date, it has not been possible to achieve single-orientation, single-variant silicon dioxide films with high piezoelectric activity. On page 827 of this issue, Carretero-Genevri *et al.* (1) demonstrate the formation of oriented piezoelectrically active α -quartz thin films directly on silicon. Although the growth mechanism and piezoelectric properties require fuller development, their approach may be an attractive route for developing integrated piezoelectric devices.

Quartz, one of 11 crystalline polymorphs of silicon dioxide, SiO₂, is the second most abundant mineral on Earth (2). Most forms of SiO₂ are composed of SiO₄ tetrahedra linked together by bridging oxygens to form a rigid three-dimensional network. The relative flexibility of the bond angles accommodates different crystalline symmetries and enhances

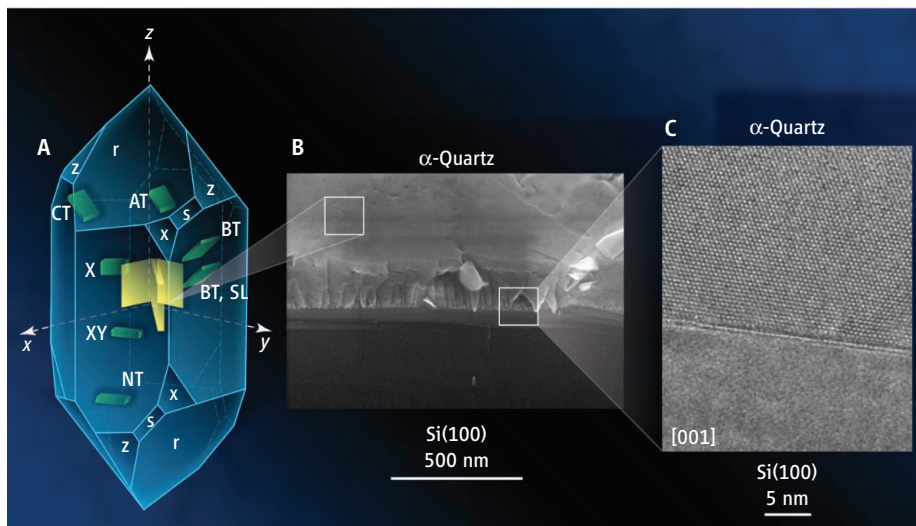
the ability of SiO₂ to form amorphous silica glass. The low-temperature form of quartz, α -quartz, possesses trigonal symmetry, a bond angle of 144°, and density of 2.65 g/cm³. Due to its high hardness, natural quartz is used as an abrasive (2). Quartz's most important technological use derives from its piezoelectric behavior (3), which is indispensable in electronics for timing control in clocks and microprocessors (4).

The piezoelectric effect, the conversion of strain into electricity (5), requires inversion asymmetry of the crystalline lattice, which is satisfied by the trigonal symmetry of α -quartz; β -quartz, which is stable above 573°C, and β -cristobalite, which is the typical devitrification (crystallization) product of amorphous silica, have hexagonal and tetrahedral symmetry, respectively, and are not piezoelectric. Although abundant, natural quartz seldom has the purity and quality needed for device applications, and almost all quartz oscillators are prepared by "slicing" bulk synthetic quartz crystals prepared hydrothermally (see the figure, panel A).

Carretero-Genevri *et al.* form α -quartz thin films directly on silicon by devitrification of amorphous Sr- or Ba-doped mesoporous

¹Department of Chemical and Nuclear Engineering, the University of New Mexico, Albuquerque, NM 87131, USA.

²Self-Assembled Materials and Electronic, Optical, and Nano Materials Departments, Sandia National Laboratories, Albuquerque, NM 87185, USA. E-mail: cjbrink@sandia.gov; pgclem@sandia.gov



Make it so. (A) Almost all quartz oscillators are prepared by slicing bulk synthetic α -quartz crystals. Common “cuts” like AT are denoted in green. (B and C) Now, highly oriented α -quartz polycrystalline films can be formed directly on Si by devitrification of amorphous mesoporous silica films (1).

silica films prepared by evaporation-induced self-assembly (6). Their process is operationally simple but mechanistically complex: Films are prepared by dip-coating from alcohol/water solutions of soluble silicic acid precursors plus surfactant or block copolymer structure-directing agents. Solvent evaporation drives the self-assembly of amorphous silica films composed of ordered arrays of macropores or large or small mesopores. Doping with $\text{Sr}(\text{NO}_3)_2$ or $\text{Ba}(\text{OH})_2$ is accomplished either in situ or in a secondary step. Heat treatment in air to 900° to 1000°C results in highly oriented α -quartz on silicon (see the figure, panel B).

Although polycrystalline, the α -quartz film bears an epitaxial relationship with the underlying (100) face of the Si substrate (see the figure, panel C), and the columnar crystallites are oriented such that there is a net piezoelectric effect. In comparison, randomly oriented or multivariant crystallites would show no net piezoelectricity, requiring thermal gradients achieved by rapid thermal processing (7) or deposition of seed layers (8) to direct oriented crystal growth.

The use of chemical, stress, and electric field gradients have also been developed as a polar variant-selective or self-polarization mechanism for LiNbO_3 and several other piezoelectric films and crystals (9). The dimensional scale of the oriented cylindrical porosity formed in the amorphous silica precursor films is more or less preserved for macroporous and large mesoporous specimens after crystallization, resulting in optically transparent, piezoelectric quartz thin films composed of oriented arrays of nanopores. In contrast, films composed of small

mesopores (around 3 nm diameter) devitrify to form dense epitaxial α -quartz films.

The detailed mechanism of the devitrification/crystallization process is presently under study, but it is sensitive to Sr or Ba, which, along with the OH content inherent to high-surface-area solution-derived amorphous silica (10), promote devitrification (11). For macroporous and large mesoporous films, devitrification is confined within the pore walls. The columnar nanoscale crystallites suggest that quartz is nucleated at the SiO_2/Si interface, where, through a heteroepitaxial relationship with Si (100), α -quartz is selected for. As crystallization proceeds from the surface by competitive growth of properly oriented crystallites, Sr or Ba as well as OH are excluded at the growth front, or conceivably at the pore walls, and transported to the film surface leaving no trace of Sr or Ba within the film or at the Si interface.

The film porosity and nanoscale dimensions of the silica pores and walls appear key to the growth mechanism. First, below a wall thickness of several nanometers, crystallization consumes the parent film to form an oriented dense α -quartz film, suggesting that the silica pore wall needs to be thicker than a critical nucleus size (or that the pore curvature be less than a critical value) to support confined/templated devitrification. Second, the transformation from amorphous silica to α -quartz is accompanied by a substantial density increase from $\sim 2.0 \text{ g/cm}^3$ to $\sim 2.65 \text{ g/cm}^3$; the thinness and weak lateral constraint of the pore wall may allow this devitrification strain to be accommodated by shrinkage of the walls as opposed to film thickness (shrinkage parallel to the substrate is precluded by coher-

ency of the quartz/Si interface). The influence of differential strain is further evident from crystallographically oriented euhedral/faceted domains that are mechanically detached along their peripheries allowing localized two-dimensional shrinkage and stress release.

The work by Carretero-Genevri \acute{e} r *et al.* represents one of the first examples of confined, heteroepitaxial devitrification to form an oriented polycrystalline film. Confined devitrification of monosized amorphous silica nanospheres to form monosized α -quartz by hydrothermal treatment in saline solutions at 200°C has been recently demonstrated (12). Whether hydrothermal processing in NaCl- or Sr^{2+} - or Ba^{2+} -containing solutions could transform macro- or mesoporous silica films to porous α -quartz remains to be seen, but such a treatment would reduce both the processing temperature and the concurrent oxidation of the Si substrate. Additionally, lithographic patterning and ink-jet printing of mesoporous silica films on Si have been reported (5, 13), and it would be of interest to demonstrate the patterned formation of porous piezoelectric quartz. Finally, detailed measurements of the piezoelectric properties of these films are needed (14). Due to their polycrystalline nature and crystallographic alignment directed by the substrate, we might expect quality factors to be inferior to those of single-crystal quartz slabs cut along preferred crystallographic angles (15). However, the coherent Si/quartz interface and film thickness combined with controlled porosity may provide advanced functionality and operational frequency range of potential interest in acoustic wave-based sensing and microelectromechanical systems.

References and Notes

1. A. Carretero-Genevri \acute{e} r *et al.*, *Science* **340**, 827 (2013).
2. J. Götze, *Mineral. Mag.* **73**, 645 (2009).
3. E. Benes *et al.*, *Sens. Actuators A Phys.* **48**, 1 (1995).
4. W. P. Mason, *J. Acoust. Soc. Am.* **70**, 1561 (1981).
5. J. Curie, P. Curie, *Bull. Soc. Minéralog. Fr.* **3**, 90 (1880).
6. Y. F. Lu *et al.*, *Nature* **389**, 364 (1997).
7. B. A. Tuttle *et al.*, *J. Am. Ceram. Soc.* **76**, 1537 (1993).
8. R. W. Schwartz *et al.*, *J. Am. Ceram. Soc.* **82**, 2359 (1999).
9. M. Houe, P. D. Townsend, *J. Phys. D Appl. Phys.* **28**, 1747 (1995).
10. C. J. Brinker, G. W. Scherer, *Sol-Gel Science: The Physics and Chemistry of Sol-Gel Processing* (Academic Press, San Diego, CA, USA, 1990).
11. W. S. Fyfe, D. S. McKay, *Am. Mineral.* **47**, 83 (1962).
12. X. Jiang *et al.*, *Chem. Commun. (Camb.)* **47**, 7524 (2011).
13. D. A. Doshi *et al.*, *Science* **290**, 107 (2000).
14. J. E. A. Southin, S. A. Wilson, D. Schmitt, R. W. Whatmore, *J. Phys. D Appl. Phys.* **34**, 1456 (2001).
15. J. Wang *et al.*, *Ultrasonics* **44** (suppl. 1), e869 (2006).

Acknowledgments: Supported by the U.S. Department of Energy Basic Energy Sciences (BES) Materials Science and Engineering Program and BES Catalysis grant DEFG02-02ER15368.

10.1126/science.1236752